Redox Biology 11 (2017) 60–72

Contents lists available at ScienceDirect

Redox Biology

journal homepage: www.elsevier.com/locate/redox

Research paper

Mitochondrial GSH replenishment as a potential therapeutic approach for Niemann Pick type C disease

Sandra Torres[a,b,1], Nuria Matías[a,b,1], Anna Baulies[a,b], Susana Nuñez[a,b], Cristina Alarcon-Vila[a,b], Laura Martinez[a,b], Natalia Nuño[a,b], Anna Fernandez[a,b], Joan Caballeria[b], Thierry Levade[c], Alba Gonzalez-Franquesa[d], Pablo Garcia-Rovés[d], Elisa Balboa[e], Silvana Zanlungo[e], Gemma Fabrías[f], Josefina Casas[f], Carlos Enrich[g,h], Carmen Garcia-Ruiz[a,b,i,*], José C. Fernández-Checa[a,b,i,*]

[a] Cell Death and Proliferation, Institute of Biomedical Research of Barcelona (IIBB), CSIC, Barcelona, Spain
[b] Liver Unit, Hospital Clinic I Provincial de Barcelona, IDIBAPS and CIBERehd, Barcelona, Spain
[c] Institut National de la Santé et de la Recherche Médicale (INSERM) UMR1037, Centre de Recherches en Cancerologie de Toulouse, Toulouse, France
[d] Diabetes and Obesity Research Laboratory, Institut d'Investigacions Biomediques August Pi i Sunyer (IDIBAPS) and Spanish Biomedical Research Centre in Diabetes and Associated Metabolic Disorders (CIBERDEM), Barcelona, Spain
[e] Departamento de Gastroenterología, Facultad de Medicina, Pontificia Universidad Católica de Chile, Santiago, Chile
[f] Research Unit on BioActive Molecules (RUBAM), Departament de Química Orgànica Biològica, Institut d'Investigacions Químiques i Ambientals de Barcelona, Consejo Superior de Investigaciones Científicas (CSIC), Barcelona, Spain
[g] Centre de Recerca Biomèdica CELLEX, Institut d'Investigacions Biomèdiques August Pi i Sunyer (IDIBAPS), 08036 Barcelona, Spain
[h] Departament de Biologia Cel·lular, Immunologia i Neurociències, Facultat de Medicina, Universitat de Barcelona, 08036 Barcelona, Spain
[i] Research Center for ALPD, Keck School of Medicine, University of Southern California, Los Angeles, CA, United States

ARTICLE INFO

Keywords:
Ceramide
Sphingolipids, Mitochondrial GSH
Cerebellum
Hepatosplenomegaly
Lysosomal disorders

ABSTRACT

Niemann Pick type C (NPC) disease is a progressive lysosomal storage disorder caused by mutations in genes encoding NPC1/NPC2 proteins, characterized by neurological defects, hepatosplenomegaly and premature death. While the primary biochemical feature of NPC disease is the intracellular accumulation of cholesterol and gangliosides, predominantly in endolysosomes, mitochondrial cholesterol accumulation has also been reported. As accumulation of cholesterol in mitochondria is known to impair the transport of GSH into mitochondria, resulting in mitochondrial GSH (mGSH) depletion, we investigated the impact of mGSH recovery in NPC disease. We show that GSH ethyl ester (GSH-EE), but not N-acetylcysteine (NAC), restored the mGSH pool in liver and brain of *Npc1*$^{-/-}$ mice and in fibroblasts from NPC patients, while both GSH-EE and NAC increased total GSH levels. GSH-EE but not NAC increased the median survival and maximal life span of *Npc1*$^{-/-}$ mice. Moreover, intraperitoneal therapy with GSH-EE protected against oxidative stress and oxidant-induced cell death, restored calbindin levels in cerebellar Purkinje cells and reversed locomotor impairment in *Npc1*$^{-/-}$ mice. High-resolution respirometry analyses revealed that GSH-EE improved oxidative phosphorylation, coupled respiration and maximal electron transfer in cerebellum of *Npc1*$^{-/-}$ mice. Lipidomic analyses showed that GSH-EE treatment had not effect in the profile of most sphingolipids in liver and brain, except for some particular species in brain of *Npc1*$^{-/-}$ mice. These findings indicate that the specific replenishment of mGSH may be a potential promising therapy for NPC disease, worth exploring alone or in combination with other options.

1. Introduction

Niemann-Pick type C (NPC) disease is an inherited lysosomal storage disorder that results in neurodegeneration, liver disease and premature death [1,2]. The juveline and most common form of the disease presents with progressive learning defects and ataxia and is typically diagnosed between 6 and 15 years of age. Mutations in genes encoding NPC1 and NPC2 proteins are causally linked to the pathology.

Abbreviations: CDX, 2-hydroxypropyl-β-cyclodextrin; GCS, glucosylceramide synthase; GSH-EE, GSH ethyl ester; mGSH, mitochondrial GSH; NAC, N-acetylcysteine; NPC, Niemann Pick type C disease; SMS, sphingomyelin synthase

* Corresponding authors at: Cell Death and Proliferation, Institute of Biomedical Research of Barcelona (IIBB), CSIC, Barcelona, Spain.
E-mail addresses: cgrbam@iibb.csic.es (C. Garcia-Ruiz), checa229@yahoo.com (J.C. Fernández-Checa).
[1] These authors contributed equally to the work.

http://dx.doi.org/10.1016/j.redox.2016.11.010
Received 13 October 2016; Received in revised form 31 October 2016; Accepted 14 November 2016
Available online 20 November 2016

Specifically, *NPC1* mutations account for 95% of cases but also alterations in *NPC2* gene have been found [2,4]. NPC1 is a transmembrane protein that binds cholesterol in its luminal N-terminal domain to allow its export, while NPC2 resides in the lysosomal lumen and transfers cholesterol to NPC1 [5]. NPC1 deficiency in mice reproduces many of the deficits seen in NPC patients, including neurological defects and ataxia by 6–7 weeks of age and reduces the maximal life span to about 10–12 weeks [2,4]. Loss of function of NPC1 causes an accumulation of free cholesterol in lysosomes and late endosomes [3,4], thereby altering intracellular transport of cholesterol. Accumulation of glycosphingolipids, especially GM2 and GM3 gangliosides, has been reported in brain of mouse models and patients [6]. NPC disease in patients and $Npc1^{-/-}$ mice is also characterized by abnormal mitochondrial function and subsequent oxidative stress [7–11]. However, the contribution of these observations to NPC disease is not well understood. For instance, treatment with antioxidants such as N-acetylcystetine (NAC), vitamin E or vitamin C, has shown little impact in modifying NPC pathology, exerting a modest effect (5–10%) in the extension of life span in $Npc1^{-/-}$ mice [7,12,13].

Impaired egress and subsequent accumulation of cholesterol in endolysosomes is the primary consequence of defective NPC1 function and is considered a major pathogenic mechanism of NPC disease [2,4]. Moreover, increased levels of cholesterol in mitochondria from liver and brain of $Npc1^{-/-}$ mice have been reported as well as [10,14,15] but the role of this event in NPC disease has not been explored. Moreover, mitochondrial cholesterol accumulation is known to decrease mitochondrial GSH (mGSH) stores by impairing cytosolic GSH transport into mitochondria [16,17]. Therefore, our aim was to address the impact of mGSH replenishment in $Npc1^{-/-}$ mice and fibroblasts from patients with NPC disease on the susceptibility to oxidant-induced cell death and NPC pathology. We show that GSH ethyl ester (GSH-EE) restores the mGSH pool and this event confers resistance to oxidative stress and cell death, improves cerebellar mitochondrial function and NPC pathology with a significant increase in the median survival and maximal life span of $Npc1^{-/-}$ mice. These findings reveal a key role of mGSH depletion in the progression of this lysosomal disorder and suggest that GSH-EE may be a promising approach for the treatment of NPC disease worth of exploring alone or in combination with existing options.

2. Materials and methods

2.1. $Npc1^{-/-}$ mice and fibroblasts from patients with NPC disease

$Npc1^{-/-}$ mice ($NPC1^{NIH}$, BALB/cJ strain) were obtained from The Jackson Laboratories. At the time of weaning (21 days), mice were genetically identified by PCR using DNA prepared from tail-tips and following the genotyping protocols provided by the supplier. All procedures involving animals and their care were approved by the Ethics Committee of the University of Barcelona and were conducted in accordance with institutional guidelines in compliance with national and international laws and policies.

Cultured human skin fibroblasts from control individuals (HSF; GM5659D) and patients with NPC disease obtained from the Laboratoire de Biochimie Metabolique, Institut Federatif de Biologie (CHU Toulouse, France) and from Coriell Institute for Medical Research (GM03123, NJ, USA) were grown at 37 °C in 5% CO_2. DMEM (Gibco) culture medium was supplemented with 10% fetal bovine serum (FBS, Gibco, 10-270-106) and 10.000 U/mL Penicillin-Streptomycin (Gibco, 15140-122).

2.2. In vitro *and* in vivo *treatments*

Primary mouse hepatocytes were isolated as described in Supplementary Methods section. Hepatocytes and fibroblasts from NPC patients were pretreated with GSH-EE (5 mM) or N-acetylcysteine (NAC, 10 mM) and then treated with hydrogen peroxide (H_2O_2, 1 mM) (Sigma) to evaluate cell viability. In addition, 7-days old $Npc1^{-/-}$ mice were treated with 1.25 mmol/kg GSH-EE (Sigma, St. Louis, MO), 2.5 mmol/Kg NAC intraperioteneally (i.p.) or vehicle (saline) every 12 h for 6 weeks to measure mGSH and total GSH levels. For survival studies, 7-days old $Npc1^{-/-}$ mice were treated with GSH-EE, NAC or vehicle every 12 h measuring body weight weekly until demise.

2.3. Cell viability assays

Cell viability was performed based on trypan blue exclusion, double staining with Hoechst 33258 as described previously [18] or by the release of Glutathione-S-Transferase as detailed in Supplemental materials and methods.

2.4. Motor coordination testing

All behavioral tests were conducted during the light cycle phase in an enclosed behavior room. Same animals were used for two motor tests, hanging test and beam transversal test, and results were evaluated and analyzed by an investigator blinded to the groups as described [19]. Briefly, hanging test was used to assess neuromuscular and locomotor development. Mice were placed on an iron wire and had to suspend their body weight with their forelimbs to avoid falling and to aid in progression around the rod. The latency to fall down and the ability to grip the wire was scored as follows: 0, mice fall immediately; 1, grips the wire with forelimbs; 2, grips the wire with forepaws and tries to support itself with its hind paws; 3, grips the wire with 3 or 4 paws; 4, grips the wire with 4 paws and twists its tail around the wire; 5, grips the wire with 4 paws, twists its tail around the wire and moves to the pole. The maximum time permitted was 60 s. Beam transversal test allows the quantification of motor deficit by measuring the time spent to arrive to the platform once all four paws of the animals are in contact with the beam (escape latency, EL), the time spent before falling (tumbled down latency, TDL) and the number of errors (NE) committed for the animals in each beam. The width of the beam was 2.5 cm and the shape was rectangular.

2.5. Mitochondria isolation and GSH determination

Mitochondrial fraction was isolated from liver and brain by Percoll density gradient centrifugation as described previously [20–22]. Mitochondrial enrichment and integrity were ascertained by the specific activity of succinic dehydrogenase and by the acceptor control ratio determined as the ADP-stimulated oxygen consumption over its absence using a Clark oxygen electrode with glutamate/malate or succinate as substrates for respiratory sites for complexes I or II. Final mitochondrial fraction was devoid of contamination by ER, plasma membrane, recycling endosomes and lysosomes as assessed by the levels of Bip/GRP78, Na^+/K^+ ATPase a1, Rab11 and acid phosphatase levels, respectively. Alternatively, primary mouse hepatocytes and fibroblasts were fractionated into cytosol and mitochondria by digitonin permeabilization as described previously [23]. In some cases, for the determination of mGSH levels the isolation buffer (250 mM sucrose, 20 mM HEPES, 1 mM EDTA, 1 mM EGTA, 1.0% (w/v) BSA, 25microl/100 mL protease inhibitor mixture, pH7.4) was supplemented with 1 mM DTT as described [24]. GSH levels in homogenates and mitochondrial fraction were determined by HPLC as described [21].

2.6. Lipidomic sphingolipid analysis

Mass spectrometry analysis of lipid species was performed in liver and brain samples from $Npc1^{-/-}$ mice with or without GSH-EE treatment. Tissue homogenates were pelleted, washed in PBS, and

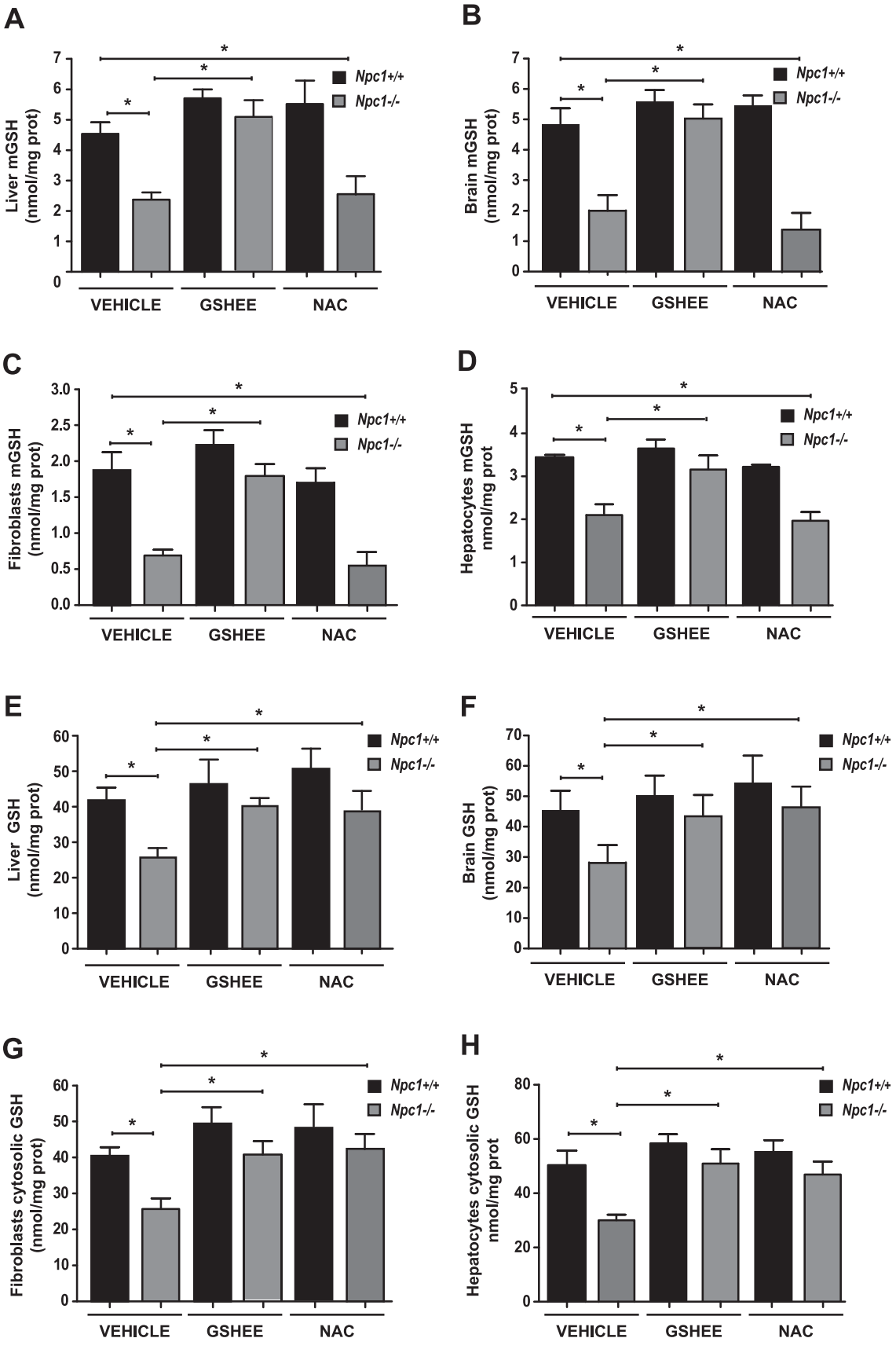
A
Liver mGSH (nmol/mg prot)
Npc1+/+
Npc1-/-
VEHICLE
GSHEE
NAC
B
Brain mGSH (nmol/mg prot)
C
Fibroblasts mGSH (nmol/mg prot)
D
Hepatocytes mGSH nmol/mg prot
E
Liver GSH (nmol/mg prot)
F
Brain GSH (nmol/mg prot)
G
Fibroblasts cytosolic GSH (nmol/mg prot)
H
Hepatocytes cytosolic GSH nmol/mg prot

transferred to glass vials. Sphingolipid extracts, spiked with internal standards (N-dodecanoylsphingosine, N-dodecanoylglucosylsphingosine, N-dodecanoylsphingosylphosphorylcholine and C17-dihydrosphingosine, 0.2 nmol each), were prepared as described [25]. The instrument consisting of a Waters Aquity UPLC system connected to a Waters LCT Premier orthogonal accelerated time of flight mass spectrometer (Waters, Millford, MA), operated in positive electrospray ionisation mode. Full scan spectra from 50 to 1500 Da were acquired and individual spectra were summed to produce data points each 0.2 s. Mass accuracy and reproducibility were maintained by using an independent reference spray by the LockSpray interference. The analytical column was a 100 mm x 2.1 mm i.d., 1.7 µm C8 Acquity UPLC BEH (Waters). The two mobile phases were phase A: water/formic acid (500/1 v/v); phase B: methanol/formic acid (500/1 v/v), both also contained 5 mM ammonium formate. A linear gradient was programmed— 0.0 min: 80% B; 3 min: 90% B; 6 min: 90% B; 15 min: 99% B; 18 min: 99% B; 20 min: 80% B. The flow rate was 0.3 mL/min. The column was maintained at 30 °C. Quantification was carried out using the extracted ion chromatogram of each compound, using 50mDa windows. The linear dynamic range was determined by injecting standard mixtures.

2.7. Tissue and fibroblasts respirometry

Fresh liver and cerebellum samples from *Npc1*$^{+/+}$, *Npc1*$^{-/-}$ and *Npc1*$^{-/-}$ mice treated with GSH-EE were homogenized mechanically with a PBI Schredder System (Pressure Biosciences, South Easton, MA, USA) [26] in MiR05 respiratory media (sucrose, 110 mM; potassium lactobionate, 60 mM; EGTA, 0.5 mM; $MgCl_2 \cdot 6H_2O$, 3 mM; taurine, 20 mM; KH_2PO_4, 10 mM; HEPES, 20 mM; BSA, 1 g/L; pH 7.1 at 37 °C). Homogenates were introduced in the 2 mL chamber of an Oroboros-2k™ respirometer (Oroboros® Instruments GmbH Corp, Austria) to perform high-resolution respirometry studies. To assess mitochondrial respiration through complex I (CI) malate (2 mM), pyruvate (5 mM) and glutamate (10 mM) were added (*leak* state) subsequently ADP+$MgCl_2$ (5 mM) and cytochrome *c* (10 mM) were titrated (*coupled* CI). Cytochrome *c* was added to assess the integrity of the membrane to rule out damage (permeabilization) of the outer mitochondrial membrane during sample preparation. To study *complex II* (CII), rotenone (0.5 mM) was added to inhibit CI before the addition of succinate (10 mM). To study *uncoupled CII*, oligomycin (2.5uM) was added to inhibit ATP synthase (or complex V, CV). *Coupled CII* respiration was calculated by substracting the *uncoupled CII* respiration from the *CII* respiration. To study the electron transport system capacity (*ETS*), subsequently the protonophore carbonyl cyanide-4-(trifluoromethoxy) phenylhydrazone (FCCP) was added in followed titrations until reaching the maximal respiration. Finally antimycin A, a complex III inhibitor, was added to inhibit respiration. The residual oxygen consumption remaining after antimycin A addition was substracted from all previous respiratory states. Protein levels were measured in the liver and cerebellum homogenates for the normalization of the different respiratory states.

Fibroblast from control subjects and patients with NPC disease were culture to determine *Routine* (R) respiration. To study un*coupled* respiration, oligomycin was added to inhibit ATP synthase. *Coupled* respiration was calculated by substracting the *uncoupled* respiration from the *routine* respiration. To study *ETS* capacity, FCCP was titrated until reaching maximal respiration. In this case, oxygen consumption values were normalized by number of cells.

2.8. Statistical analyses

Statistical analyses were performed using GraphPad Prism 6 (Graphpad Software Inc). Unpaired Student's *t*-test (two tailed) was performed between two groups and one or two-way ANOVA followed by Tukey's Multiple Comparison test were used for statistical comparisons between three or more groups. Kaplan-Meier survival curves were plotted using the GraphPad Prism and the log-rank test was undertaken to determine the statistical significance. The corresponding number of experiments is indicated in the figure legends. Data in graphs are shown as mean ± s.e.m.

3. Results

3.1. GSH-EE treatment but not NAC restores mGSH levels in liver and brain from Npc1$^{-/-}$ mice and fibroblasts from NPC patients

Besides endolysosomes, cholesterol has been shown to accumulate in hepatic and brain mitochondria of *Npc1*$^{-/-}$ mice [10,14,15]. Consistent with the impairment of mitochondrial GSH transport by cholesterol [15–17,27], liver and brain mitochondria from *Npc1*$^{-/-}$ mice exhibited decreased mGSH levels compared to *Npc1*$^{+/+}$ mice (Fig. 1A, B). Similar findings were observed in mitochondria from fibroblasts of NPC patients (Fig. 1C), which also exhibit increased mitochondrial cholesterol loading [9]. To address the potential impact of mGSH depletion in NPC disease, we first examined strategies to recover mGSH levels. The pool of mGSH derives from the transport of cytosolic GSH into the mitochondrial matrix [17,28]. Although NAC provides cysteine, the rate-limiting amino acid needed for GSH neosynthesis in the cytosol, mitochondrial cholesterol accumulation impairs the transport of the newly synthesized cytosolic GSH into mitochondria due to the cholesterol-dependent decrease of mitochondrial membrane fluidity, as reported in steatohepatitis, anthrax infection and Alzheimer's disease [14,16,27,29–32]. GSH ethyl ester (GSH-EE), on the other hand, freely crosses membrane bilayers and diffuses into mitochondria resulting in mGSH replenishment. Indeed, GSH-EE has been shown to increase mGSH levels in cerebral cortex from newborn rats [33] and to protect against TNF-induced hepatocellular apoptosis and diet-mediated steatohepatitis [16,17,32]. Therefore, we examined the effect of *in vivo* treatment of *Npc1*$^{-/-}$ mice with GSH-EE. As seen, intraperitoneal (i.p.) treatment of *Npc1*$^{-/-}$ mice at postnatal day 7 (P7) every 12 h with GSH-EE restored mGSH levels in liver and brain mitochondria (Fig. 1A, B) as well as in isolated hepatocytes from *Npc1*$^{-/-}$ mice (Fig. 1D). Similar replenishment of mGSH by GSH-EE was observed in fibroblasts from patients with NPC disease (Fig. 1C). In line with these findings, GSH-EE increased total GSH levels in *Npc1*$^{-/-}$ mice as well as in fibroblasts of NPC patients (Fig. 1E-H). In contrast, *in vivo* treatment with NAC at p7 failed to replenish mGSH stores in affected organs of *Npc1*$^{-/-}$ mice or fibroblasts from NPC patients (Fig. 1A-D), although it efficiently increased total GSH levels, in agreement with previous findings [7]. GSH-EE treatment, however, did not prevent the accumulation of cholesterol in mitochondria

Fig. 1. Effect of GSH-EE or NAC therapy on GSH homeostasis in NPC disease. *Npc1*$^{-/-}$ mice were treated with saline (vehicle), GSHEE or NAC at postnatal day 7 every 12 h for 6 weeks to isolate mitochondria from liver and brain. (**A**) GSH levels in mitochondria from liver and (**B**) GSH levels in mitochondria from brain. Values are compared to liver and brain mitochondria from *Npc1*$^{+/+}$ mice. Data are presented as means ± SEM (n=3 to 11, P < 0.05, two-way ANOVA and Tukey's Multiple Comparison Post-test). (**C**) GSH levels in mitochondria from fibroblasts from control subjects (NPC$^{+/+}$) or NPC patients (NPC$^{-/-}$) incubated in vitro with GSH-EE (5 mM) or NAC (10 mM). Data are presented as means ± SEM (n=3 to 6, P < 0.05, two-way ANOVA and Tukey's Multiple Comparison Post-test). (**D**) Mitochondrial GSH in hepatocytes from *Npc1*$^{+/+}$ mice and *Npc1*$^{-/-}$ mice treated or not with GSH-EE or NAC as in (A). Data are presented as means ± SEM (n=3, P < 0.05, two-way ANOVA and Tukey's Multiple Comparison Post-test). Total GSH levels from liver (**E**) or brain (**F**) homogenates of *Npc1*$^{+/+}$ mice and *Npc1*$^{-/-}$ mice treated with saline (vehicle), GSHEE or NAC. Data are presented as means ± SEM (n=5–7, P < 0.05, two-way ANOVA and Tukey's Multiple Comparison Post-test). Total GSH levels of homogenates from hepatocytes from *Npc1*$^{+/+}$ mice and *Npc1*$^{-/-}$ mice (**G**) or fibroblasts from control subjects or NPC patients (**H**) treated with GSH-EE, NAC or saline. Data are means ± SEM (n=5–7, P < 0.05, two-way ANOVA and Tukey's Multiple Comparison Post-test).

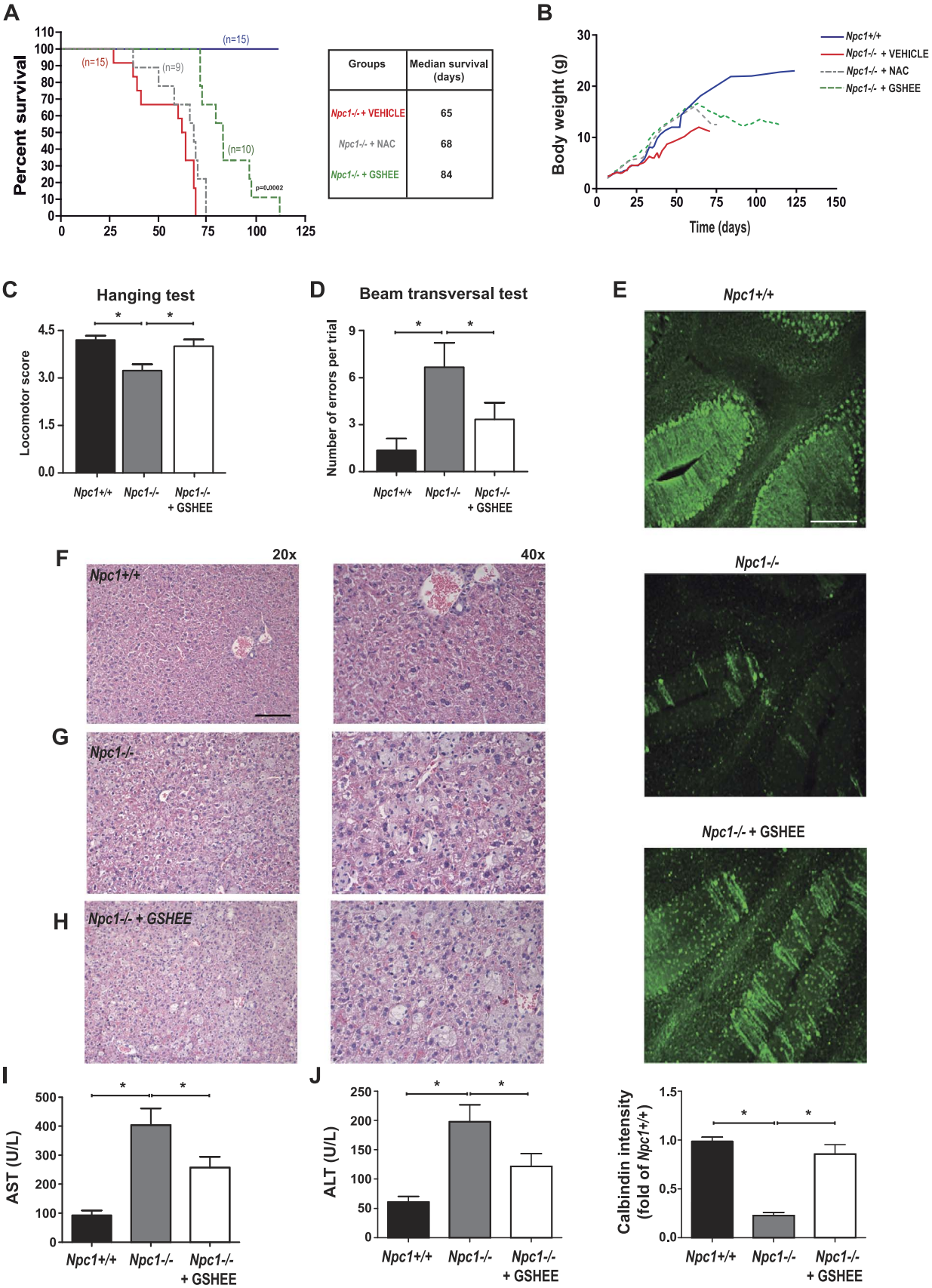
A
Percent survival
(n=15)
(n=15)
(n=9)
(n=10)
p=0.0002
Groups
Median survival (days)
Npc1-/- + VEHICLE
65
Npc1-/- + NAC
68
Npc1-/- + GSHEE
84
B
Body weight (g)
Time (days)
Npc1+/+
Npc1-/- + VEHICLE
Npc1-/- + NAC
Npc1-/- + GSHEE
C
Hanging test
Locomotor score
Npc1+/+
Npc1-/-
Npc1-/- + GSHEE
D
Beam transversal test
Number of errors per trial
Npc1+/+
Npc1-/-
Npc1-/- + GSHEE
E
Npc1+/+
Npc1-/-
Npc1-/- + GSHEE
F
20x
40x
Npc1+/+
G
Npc1-/-
H
Npc1-/- + GSHEE
I
AST (U/L)
Npc1+/+
Npc1-/-
Npc1-/- + GSHEE
J
ALT (U/L)
Npc1+/+
Npc1-/-
Npc1-/- + GSHEE
Calbindin intensity (fold of Npc1+/+)
Npc1+/+
Npc1-/-
Npc1-/- + GSHEE

isolated from liver and brain from *Npc1*$^{-/-}$ mice (21 ± 3 vs 25 ± 4 μg cholesterol/mg protein in liver mitochondria from *Npc1*$^{-/-}$ and *Npc1*$^{-/-}$+GSH-EE groups, respectively, and 35 ± 6 vs 32 ± 5 μg cholesterol/mg protein in brain mitochondria from *Npc1*$^{-/-}$ and *Npc1*$^{-/-}$+GSH-EE groups, respectively), suggesting that the recovery of mGSH by GSH-EE is independent of cholesterol-mediated impairment in the transport of GSH into mitochondria. These findings show that unlike NAC, GSH-EE is capable of restoring mGSH pool in *Npc1*$^{-/-}$ mice and in fibroblasts from NPC patients.

3.2. Intraperitoneal GSH-EE therapy improves NPC pathology and extends the survival of Npc1$^{-/-}$ mice

Premature death is a characteristic feature of NPC disease, and hence we next examined the survival of *Npc1*$^{-/-}$ mice following GSH-EE and NAC treatment *in vivo*. Although somewhat lower than reported in some studies [34,35], the median survival and maximal life span of our vehicle-treated *Npc1*$^{-/-}$ colony were in line with previous reports [19,36,37]. As seen, intraperitoneal GSH-EE therapy significantly extended the median survival and increased the maximum life span of *Npc1*$^{-/-}$ mice with respect to vehicle-treated *Npc1*$^{-/-}$ mice (Fig. 2A), similar to the effect we observed following subcutaneous treatment of *Npc1*$^{-/-}$ mice with 2-hydroxypropyl-β-cyclodextrin (CDX), an agent that extracts cholesterol from membrane bilayers [34], or CDX plus GSH-EE (Torres et al, mansucript in preparation). Moreover, GSH-EE-treated *Npc1*$^{-/-}$ mice maintained a significantly higher body weight compared to vehicle-treated *Npc1*$^{-/-}$ mice, while *Npc1*$^{-/-}$ mice treated with NAC exhibited somewhat lower body weight gain (Fig. 2B). Consistent with the inability of NAC to replenish mGSH levels, intraperitoneal NAC therapy did not have a significant impact in the survival of *Npc1*$^{-/-}$ mice (Fig. 2A), in agreement with previous observations [7].

As NPC disease causes neurodegeneration, with characteristic signs of cerebellar ataxia, and liver disease, we next addressed the pathological impact of mGSH replenishment by GSH-EE. GSH-EE treatment improved motor coordination assessed by the hanging and beam transversal tests (Fig. 2C, D). Consistent with this outcome, the levels of calbindin, a calcium-binding protein critical for the precision of motor coordination [38], were reduced in cerebellar Purkinje cells from *Npc1*$^{-/-}$ mice while GSH-EE treatment significantly increased calbindin expression (Fig. 2E). Moreover, *Npc1*$^{-/-}$ mice exhibited age-dependent liver injury assessed by serum ALT levels that was evident 7 weeks after birth (Supplementary Fig. 1). H & E analyses indicated alterations in liver parenchyma with the presence of inflammatory foci, bigger and more irregular hepatocytes with foamy cytoplasm, suggesting lipid accumulation (Fig. 2F). In addition, compared to vehicle-treated Npc1$^{-/-}$ mice GSH-EE therapy at P7 significantly decreased liver damage as indicated by H & E analyses (Fig. 2 G, H) and decreased levels of serum transaminases (Fig. 2 I, J). Thus, these findings underscore that GSH-EE therapy ameliorates NPC pathology and increases the survival of *Npc1*$^{-/-}$ mice.

3.3. GSH-EE treatment protects against oxidative stress in Npc1$^{-/-}$ mice and fibroblasts from patients with NPC disease

Given the lack of therapeutic effect of NAC in the survival of *Npc1*$^{-/-}$ mice, we next examined potential mechanisms underlying the beneficial effect of mGSH replenishment by GSH-EE treatment. As NPC disease is characterized by oxidative stress [7,11], we first examined the susceptibility to oxidant-induced cell death. As seen, GSH-EE treatment protected isolated hepatocytes from *Npc1*$^{-/-}$ mice and fibroblasts from NPC patients against hydrogen peroxide-induced cell death (Fig. 3A, B). In line with these findings, *in vivo* treatment of *Npc1*$^{-/-}$ mice with GSH-EE decreased oxidative stress in liver and cerebellum as revealed by reduced carbonylated proteins (Fig. 3C, D). Moreover, GSH-EE administration attenuated the increase of MitoSOX™ fluorescence in hepatocytes isolated from *Npc1*$^{-/-}$ mice (Fig. 3E), indicating reduced generation of superoxide anion, while GSH-EE treatment increased mitochondrial membrane potential (Fig. 3F). Furthermore, GSH-EE therapy significantly increased ATP levels in liver and cerebellum from *Npc1*$^{-/-}$ mice (Supplementary Fig. 2), suggesting improved energy status. Furthermore, *Npc1*$^{-/-}$ mice exhibited increased caspase-3 processing to active fragment in liver and cerebellum and GSH-EE treatment decreased caspase 3 activity (Fig. 3G, H). Moreover, increased plasma levels of cholesterol oxidation products have been identified as sensitive and specific markers of NPC disease [39]. In line with these findings, we observed increased plasma levels of the oxysterols cholestane 3β, 5α, 6β-triol and 7-ketocholesterol, which were differentially affected by GSH-EE treatment (Supplementary Fig. 3). NPC disease most severely affects Purkinje cells of the cerebellum. As seen, nitrotyrosine immunohistochemical analysis of cerebellar frozen sections indicated marked nitrotyrosylation in granule and Purkinje cells from *Npc1*$^{-/-}$ mice compared to *Npc1*$^{+/+}$ mice (Fig. 3I). Interestingly, GSH-EE treatment reduced protein nitrotyrosylation in cerebellar slices from *Npc1*$^{-/-}$ mice (Fig. 3I). Thus, these findings indicate that GSH-EE therapy attenuates the susceptibility to oxidative stress and cell death in NPC disease.

3.4. GSH-EE therapy improves mitochondrial function in cerebellum from Npc1$^{-/-}$ mice

As mitochondria are one of the main culprits of ROS overgeneration leading to oxidative stress, we next evaluated the effects of GSH-EE treatment in mitochondrial function and morphology. High-resolution respirometry analyses were performed in homogenates from cerebellum of *Npc1*$^{-/-}$ mice with or without i.p. GSH-EE treatment. Oxygen consumption rate assessed at the leak state (no ADP, state 2 respiration) in the presence of malate and glutamate (complex I substrates) was similar in the cerebellum of *Npc1*$^{+/+}$ and *Npc1*$^{-/-}$ mice and was not affected upon GSH-EE treatment (Fig. 4A). However, oxidative phosphorylation through complex I in the presence of ADP was reduced in cerebellum of *Npc1*$^{-/-}$ mice, and this effect was recovered by GSH-EE treatment (Fig. 4A). GSH-EE treatment caused similar effects when the respiratory capacity was evaluated in the presence of rotenone (complex I inhibitor) and succinate (complex II substrate) and with the addition of the ATP synthase inhibitor oligomycin and the pronotophore FCCP to monitor coupled respiration and the maximal electron transfer System (ETS), respectively (Fig. 4B). A similar outcome was observed in liver homogenates of *Npc1*$^{-/-}$ mice compared to *Npc1*$^{+/+}$ mice, but unlike in cerebellum, GSH-EE treatment failed to restore leak respiration, oxidative phosphorylation via complex I and II as well as coupled and ETS respiration via complex II (Supplementary

Fig. 2. Intraperitoneal treatment with GSH-EE improves NPC pathology and extends survival of Npc1$^{-/-}$ mice. (**A**) Kaplan-Meier survival plots and medium survival of *Npc1*$^{-/-}$ mice treated with GSH-EE, NAC or saline (vehicle) at P7 every 12 h. P < 0.0002 vs. Npc1$^{-/-}$ mice treated with NAC or vehicle. (**B**) Effect of GSH-EE or NAC therapy in body weight gain of *Npc1*$^{-/-}$ mice. Mice were treated as in (A) and body weight was recorded weekly until demise. (**C**) Hanging test and (**D**) beam transversal test in *Npc1*$^{-/-}$ mice treated with vehicle or GSH-EE at p7 every 12 h for 6 weeks. Data are presented as means ± SEM (n=7 to 13, P < 0.05 vs. *Npc1*$^{+/+}$ mice or *Npc1*$^{-/-}$ mice, one-way ANOVA and Tukey's Multiple Comparison Post-test). (**E**) Calbindin immunostaining in cerebellar paraffined sections of *Npc1*$^{+/+}$ mice and *Npc1*$^{-/-}$ mice following treatment with saline (vehicle) or GSH-EE. Images are representative of 5 replicates showing similar results. **(F-H)** Liver sections from *Npc1*$^{+/+}$ mice and *Npc1*$^{-/-}$ mice treated with saline or GSH-EE analyzed by H & E. Representative images of 6 replicates are shown. (**I, J**) Serum ALT levels from *Npc1*$^{+/+}$ mice and *Npc1*$^{-/-}$ mice treated with saline or GSH-EE. Data are presented as means ± SEM (n=7 to 14, P < 0.05 vs. *Npc1*$^{+/+}$ mice or *Npc1*$^{-/-}$ mice, one-way ANOVA and Tukey's Multiple Comparison Post-test).

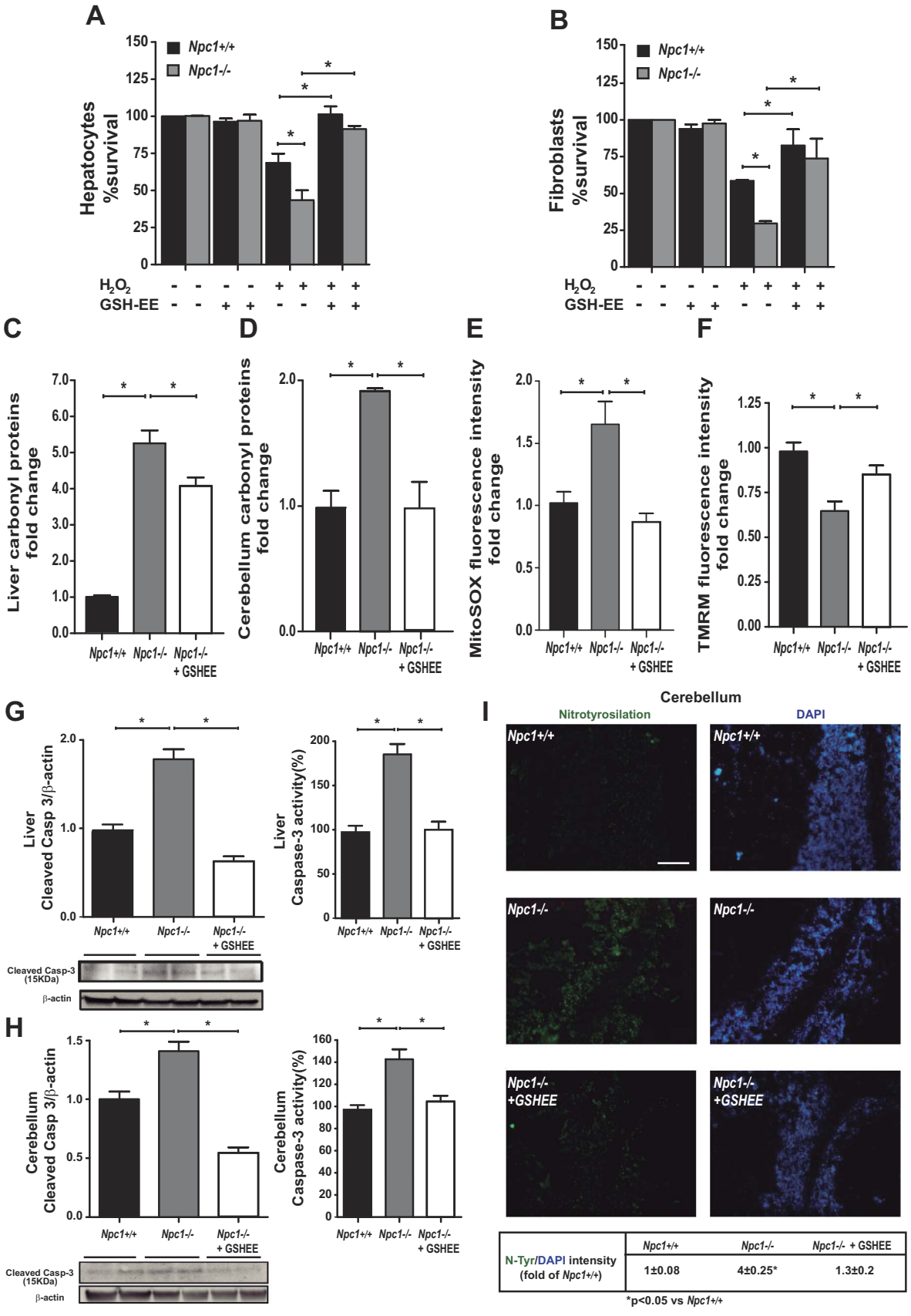

	Npc1+/+	Npc1-/-	Npc1-/- + GSHEE
N-Tyr/DAPI intensity (fold of Npc1+/+)	1±0.08	4±0.25*	1.3±0.2

*p<0.05 vs Npc1+/+

Fig. 4). Fibroblasts from patients with NPC disease showed a significant reduction in mitochondrial performance at routine, coupled and ETS respiratory states compared to fibroblasts from healthy subjects (Supplementary Fig. 5). These findings of mitochondrial respiratory rates in liver and cerebellum correlate with the expression of mitochondrial complexes (Fig. 4C). Blue native electrophoresis revealed significant downregulation of supercomplexes I_1+III_2+IV_2 and, particularly, complex IV in liver but not cerebellum of *Npc1*$^{-/-}$ mice that was not reversed by GSH-EE treatment, with modest differences observed regarding complex CIV levels in cerebellum (Fig. 4C). Western blot analyses revealed decreased expression of the mitochondrial DNA (mtDNA)-encoded subunit of the CIV cytochrome c oxidase I in liver but not cerebellum that was not prevented by GSH-EE treatment (Supplementary Fig. 6). Moreover, electron microscopy analyses showed autophagic vacuoles of electron-dense materials, mitochondrial morphological alterations predominantly in liver with decreased mitochondrial number and increased length (Supplemental Fig. 7) without a significant effect following GSH-EE treatment. In contrast to the liver, the mitochondrial structure and number in cerebellum was similar between *Npc1*$^{+/+}$ and *Npc1*$^{-/-}$ mice and GSH-EE treatment increased the mitochondrial length in *Npc1*$^{-/-}$ mice (Fig. 4D, E). Overall, these findings point to reversible functional mitochondrial alterations in cerebellum of *Npc1*$^{-/-}$ mice, which are largely restored by GSH-EE treatment, suggesting the involvement of an oxidative stress-dependent mechanism of mitochondrial dysfunction. The mitochondrial alteration in liver of *Npc1*$^{-/-}$ mice likely reflects structural defects with decreased expression of mtDNA-encoded subunits and assembly of mitochondrial complexes that are refractory to GSH-EE administration.

3.5. Effect of GSH-EE therapy in the shingolipidomic profile of liver and brain from Npc1$^{-/-}$ mice

In addition to cholesterol, NPC disease is also characterized by the accumulation of sphingolipids in the affected organs [6]. Therefore, we next addressed whether GSH-EE treatment induced major changes in the sphingolipidomic profile in liver and brain of *Npc1*$^{-/-}$ mice. As seen, mass spectrometry analysis revealed increased levels of specific molecular species of ceramide, sphingomyelin, monohexosylceramide (glucosyl and galactosylceramides), dihexosylceramide (lactosylceramides) and sphingosine in liver of *Npc1*$^{-/-}$ mice (Fig. 5). The increase of sphingolipids in brain of *Npc1*$^{-/-}$ mice was evident for ceramide C18:0, dihexosylceramides C18GGCer and C20GGCer and sphingosine (Fig. 6). In contrast to these findings, the levels of specific sphingomyelin (C22SM, C24SM, C24:1SM and C24:2SM) and, particularly, the most predominant monohexosylceramide species (C18GCer, C20GCer, C22GCer, C24GCer and C24:1GCer) decreased in brain of *Npc1*$^{-/-}$ mice compared to *Npc1*$^{+/+}$ mice (Fig. 6), in agreement with previous findings [6]. These changes in sphingolipid homeostasis were accompanied by unchanged expression of glucosylceramide synthase (GCS) and sphingomyelin synthase (SMS) 2 in liver and brain, while that of SMS 1 decreased in liver (Fig. 7). Interestingly, the sphingolipidomic profile of the liver from *Npc1*$^{-/-}$ mice treated with GSH-EE was similar to that of vehicle-treated *Npc1*$^{-/-}$ mice (Fig. 5). Moreover, GSH-EE treatment did not significantly change the profile of ceramide, dihexosides species or sphingosine levels in brain of *Npc1*$^{-/-}$ mice, except for the normalization of specific molecular species of sphingomyelin and monohexosylceramides in the brain of *Npc1*$^{-/-}$ mice (Fig. 6). These findings underscore that GSH-EE therapy has a modest and selective effect on the sphingolipid profile in *Npc1*$^{-/-}$ mice.

4. Discussion

The primary biochemical feature of NPC disease is the accumulation of free cholesterol, predominantly in endolysosomes, due to defective NPC1 function. Also described but poorly characterized is the increase of cholesterol in mitochondria in the affected organs of *Npc1*$^{-/-}$ mice. As mitochondrial cholesterol accumulation depletes the mGSH pool [14,15], we examined for the first time the impact of mGSH replenishment in NPC disease. Our findings show a differential outcome between NAC and GSH-EE in the compartimentalization of GSH in NPC disease. Incubation of hepatocytes from *Npc1*$^{-/-}$ mice and fibrosblasts of NPC patients with NAC and GSH-EE results in a significant increase in total GSH levels. Moreover, consistent with the ability to cross the blood brain barrier [14,33], *in vivo* treatment with both precursors increased total GSH levels in liver and brain homogenates from *Npc1*$^{-/-}$ mice, in agreement with previous findings [7]. However, unlike GSH-EE, NAC failed to restore the mGSH pool despite significantly increasing total GSH levels. The inability of NAC to increase mGSH in NPC disease is in line with findings in liver and alveolar type II cells following chronic alcohol drinking [20,23,40], which causes increased mitochondrial cholesterol loading [41,42] and subsequent impairment in the transport of GSH from the cytosol into mitochondria through disruption of membrane dynamics. Interestingly, we show that the proficiency of NAC to restore total GSH levels but not the mGSH pool had little impact in the survival of *Npc1*$^{-/-}$ mice or NPC pathology, in line with previous studies [7,43]. Accordingly, short-term NAC administration to NPC patients revealed no significant effects on oxidative stress [7]. In addition, vitamin C treatment did not significantly modify disease progression nor increased life span of *Npc1*$^{-/-}$ mice [13]. Thus, while oxidative stress is a characteristic feature of NPC disease, treatment with antioxidants or replenishment of total GSH levels is not an efficient approach to modify disease progression.

The present findings provide evidence that selective restoration of mGSH following GSH-EE therapy has a promising therapeutic impact in NPC disease, significantly preserving calbindin levels, improving motor coordination and increasing the survival of *Npc1*$^{-/-}$ mice. While GSH-EE treatment increased mGSH levels in both liver and cerebellum, the normalization of mitochondrial function was only observed in the latter, which paralleled the improvement of Purkinje cell survival and protection against oxidative stress, likely mediating the enhanced motor coordination and increased survival. Recent observations indicated that the hepatic re-expresion of NPC1 in *Npc1*$^{-/-}$ mice corrects the liver phenotype of the disease, although, this outcome had no impact in improving neurological symptoms or life-span extension

Fig. 3. GSE-EE protects against oxidative stress and cell death in Npc1$^{-/-}$ mice and fibroblasts from NPC patients. (**A**) Survival of hepatocytes from *Npc1*$^{+/+}$ mice and *Npc1*$^{-/-}$ mice following treatment with GSH-EE (5 mM) challenged with hydrogen peroxide (1 mM). Data are presented as means ± SEM (n=3 to 4, $P < 0.05$, two-way ANOVA and Tukey's Multiple Comparison Post-test). (**B**) Susceptibility of fibroblasts from control (NPC$^{+/+}$) or NPC patients (NPC$^{-/-}$) to hydrogen peroxide treatment. Data are presented as mean ± SEM (n=3, $P < 0.05$, two-way ANOVA and Tukey's Multiple Comparison Post-test). (**C**) Protein carbonylation from liver or brain (**D**) of *Npc1*$^{+/+}$ mice or *Npc1*$^{-/-}$ mice treated with saline or GSH-EE at p7 every 12 h for 6 weeks. Data are presented as means ± SEM (n=3 to 6, $P < 0.05$ vs. *Npc1*$^{+/+}$ mice or *Npc1*$^{-/-}$ mice as indicated, one-way ANOVA and Tukey's Multiple Comparison Post-test). (**E**) MitoSOX fluorescence of isolated hepatocytes from *Npc1*$^{+/+}$ mice or *Npc1*$^{-/-}$ mice treated with saline or GSH-EE. Data are presented as means ± SEM (n=5 to 10, $P < 0.05$ vs. Npc1$^{+/+}$ or Npc1$^{-/-}$ mice, one-way ANOVA and Tukey's Multiple Comparison Post-test). (**F**) TMRM fluorescence of isolated hepatocytes from *Npc1*$^{+/+}$ mice or *Npc1*$^{-/-}$ mice treated saline or GSH-EE. Data are presented as means ± SEM (n=7 to 11, $P < 0.05$ vs. Npc1$^{+/+}$ or Npc1$^{-/-}$ mice, one-way ANOVA and Tukey's Multiple Comparison Post-test). (**G**) Active caspase-3 fragment of liver or cerebellum (**H**) from *Npc1*$^{+/+}$ mice or *Npc1*$^{-/-}$ mice treated saline or GSH-EE. Representative western showing the 15KDa fragment. Data are presented as means ± SEM (n=3, $P < 0.05$ vs. Npc1$^{+/+}$ or Npc1$^{-/-}$ mice, one-way ANOVA and Tukey's Multiple Comparison Post-test). (**I**) Nitrotyrosine immunohistochemical determination in cerebellar frozen sections (12 μm) and DAPI staining to identify nuclei of Purkinje cells. Representative images of 4 replicates of *Npc1*$^{+/+}$ and *Npc1*$^{-/-}$ mice treated or not with GSH-EE. Scale bar represents 200 μm.

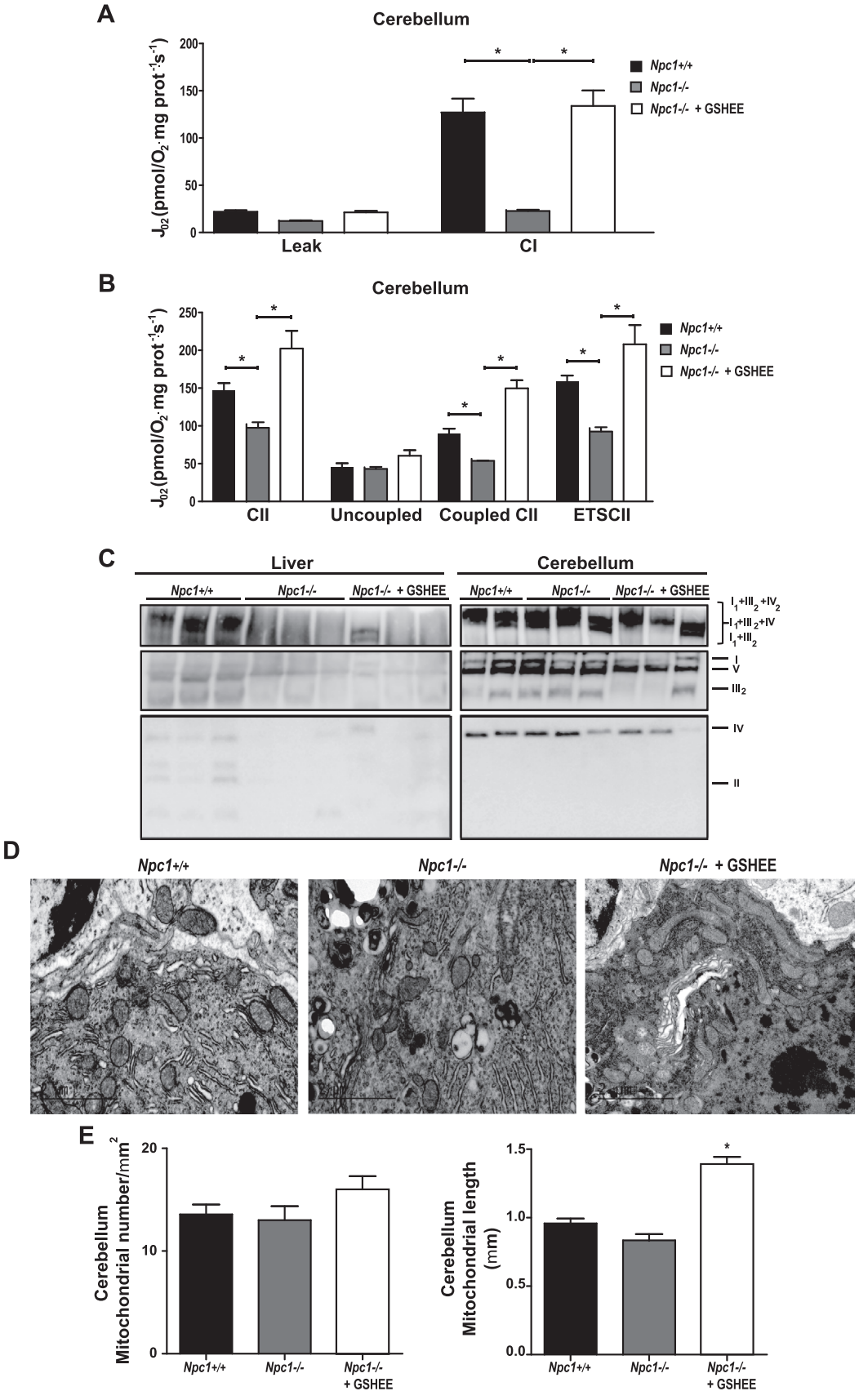
A
Cerebellum
J_{02}(pmol/O_2·mg prot·$^{-1}$s^{-1})
200
150
100
50
0
*
*
Npc1+/+
Npc1-/-
Npc1-/- + GSHEE
Leak
CI
B
Cerebellum
J_{02}(pmol/O_2·mg prot·$^{-1}$s^{-1})
250
200
150
100
50
0
*
*
*
*
*
*
Npc1+/+
Npc1-/-
Npc1-/- + GSHEE
CII
Uncoupled
Coupled CII
ETSCII
C
Liver
Cerebellum
Npc1+/+
Npc1-/-
Npc1-/- + GSHEE
Npc1+/+
Npc1-/-
Npc1-/- + GSHEE
I_1+III_2+IV_2
I_1+III_2+IV
I_1+III_2
I
V
III_2
IV
II
D
Npc1+/+
Npc1-/-
Npc1-/- + GSHEE
E
Cerebellum Mitochondrial number/mm^2
20
10
0
Npc1+/+
Npc1-/-
Npc1-/- + GSHEE
Cerebellum Mitochondrial length (mm)
1.5
1.0
0.5
0.0
*
Npc1+/+
Npc1-/-
Npc1-/- + GSHEE

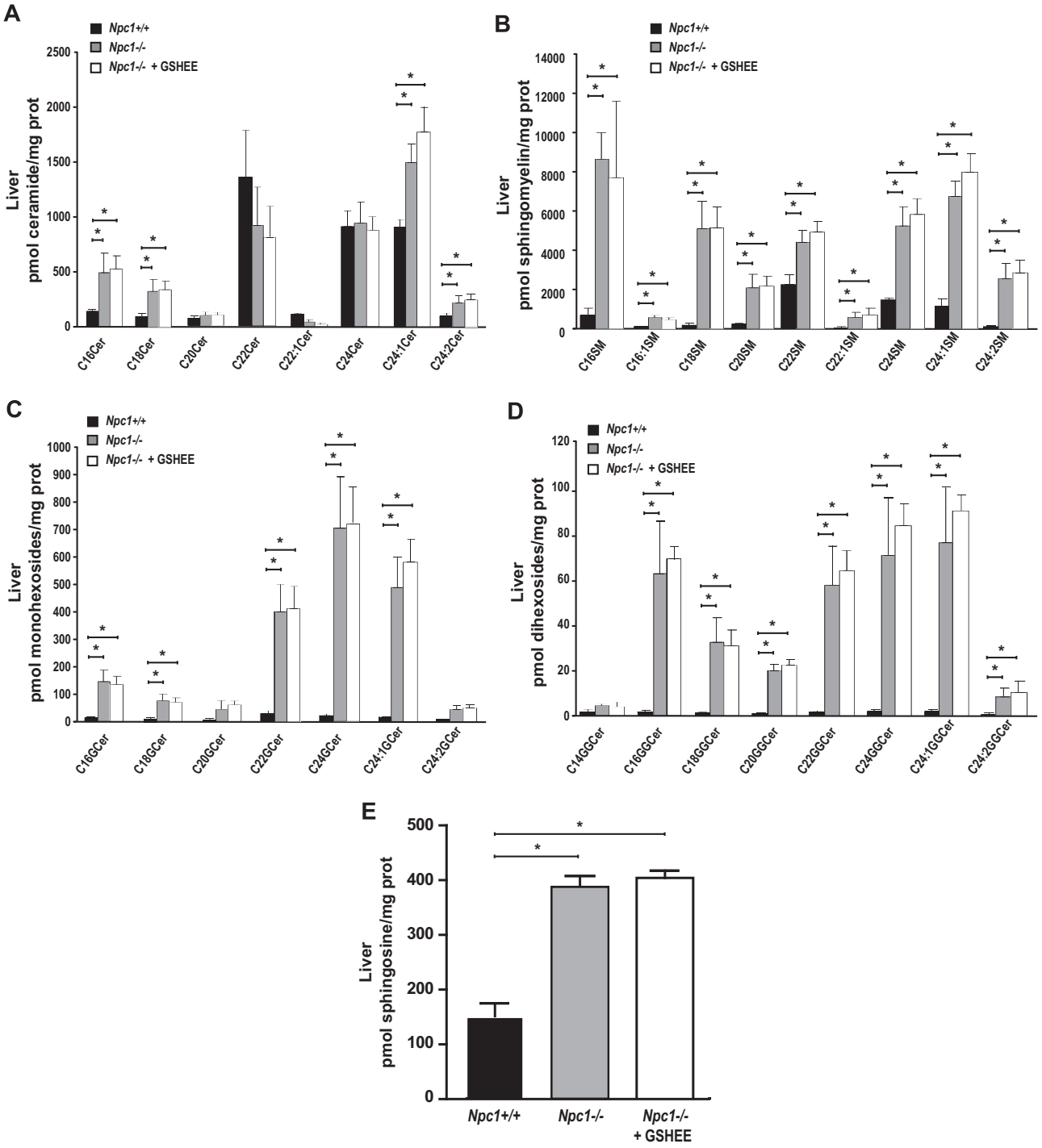

Fig. 5. Mass spectrometry analyses of hepatic sphingolipid profile of *Npc1*$^{-/-}$ mice. Liver samples from *Npc1*$^{+/+}$ mice and *Npc1*$^{-/-}$ mice treated with saline or GSH-EE at p7 every 12 h for 6 weeks were processed for lipidomic analyses of ceramide (**A**); sphingomyelin (**B**); monohexosides (**C**); dihexosides (**D**) species and sphingosine (**E**) levels. Values are the mean ± SEM of 5 mice per group. $P < 0.05$ vs. *Npc1*$^{+/+}$ or *Npc1*$^{-/-}$ samples as indicated.

Fig. 4. High-resolution respirometry of cerebellum from Npc1$^{-/-}$ mice treated with GSH-EE. Cerebellar homogenates of *Npc1*$^{+/+}$ mice or *Npc1*$^{-/-}$ mice treated with saline or GSH-EE were analyzed in Oroboros-2k™ respirometer. (**A**) For mitochondrial respiration through complex I, malate 2 mM, pyruvate 5 mM and glutamate 10 mM were added with or without ADP+$MgCl_2$ (5 mM) to determine respiration at couple or leak states, respectively. Data are presented as means ± SEM (n=3 to 7, $P < 0.05$ vs. Npc1$^{+/+}$ or Npc1$^{-/-}$ mice, one-way ANOVA and Tukey's Multiple Comparison Post-test). (**B**) Oxidative phosphorylation through complex II was determined using succinate (10 mM) as substrate in the presence of rotenone (0.5 mM). Uncoupled respiration through complex II was determined in the presence of oligomycin (2.5 μM) and the electron transport System capacity was determined in the presence of FCCP. Coupled respiration was calculated by substracting the uncoupled respiration from the respiration through complex II. Data are presented as means ± SEM (n=3 to 7, $P < 0.05$ vs. Npc1$^{+/+}$ or Npc1$^{-/-}$ mice, one-way ANOVA and Tukey's Multiple Comparison Post-test). (**C**) Blue native Page electrophoresis of liver and cerebellum *Npc1*$^{+/+}$ or *Npc1*$^{-/-}$ mice treated or not with GSH-EE to detect OXPHOS complexes with Total Mitoprofile OXPHOS Rodent antibody cocktail. Images are representative of 4 replicates per group. (**D**) Electron microscopy analyses of cerebellum from *Npc1*$^{+/+}$ or *Npc1*$^{-/-}$ mice with or without GSH-EE that were transcardially washed with cold saline before perfusion with 2.5% glutaraldehyde. Images were acquired with a Gatan Orius digital camera and are representative of 5 replicates per group. (**E**) Mitochondrial number and length of cerebellar samples were quantified from images of ultrathin sections from (**D**) acquired by moving at random across the EM grid (two grids per animal) and analyzed using the iTEM program and ImageJ software. Data are presented as means ± SEM (n=4 to 7, $P < 0.05$ vs. Npc1$^{+/+}$, one-way ANOVA and Tukey's Multiple Comparison Post-test).

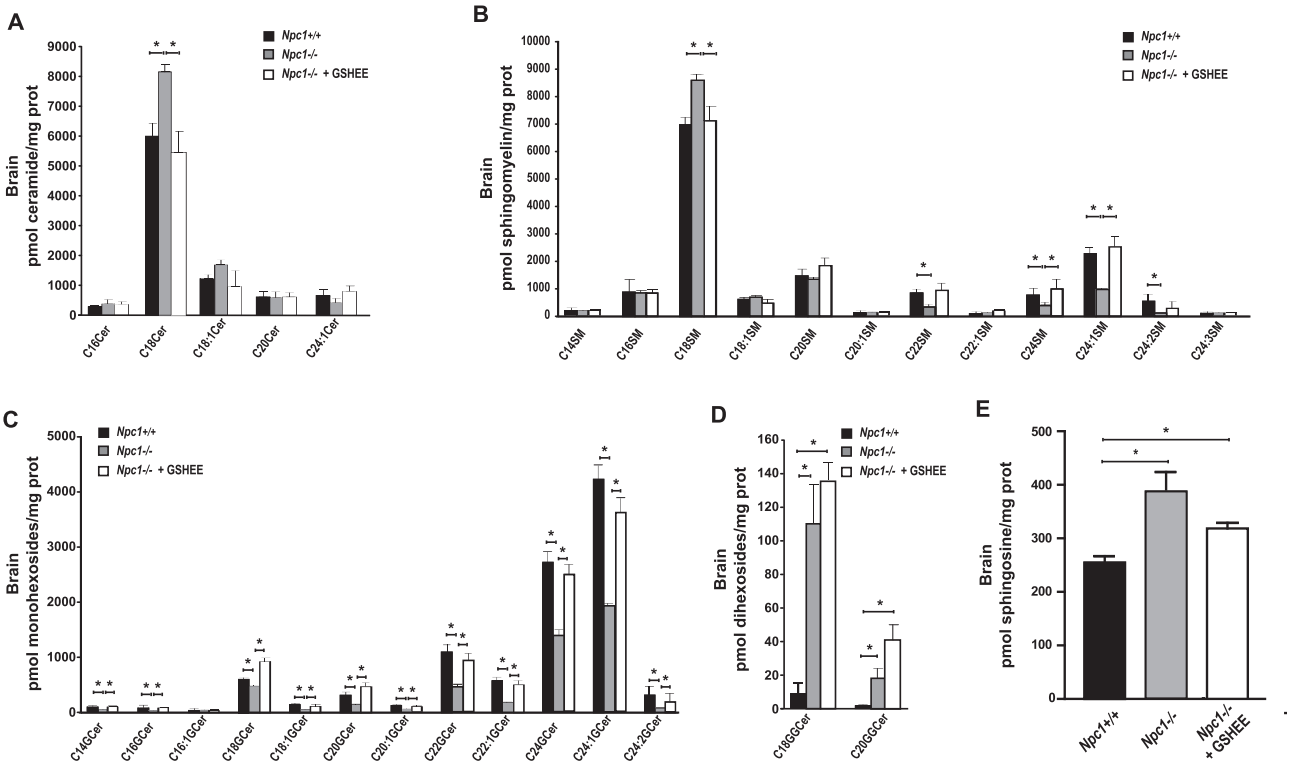

Fig. 6. Sphingolipidomic profile of brain of NPC1$^{-/-}$ **mice**. Brain samples from *Npc1*$^{+/+}$ mice and *Npc1*$^{-/-}$ mice treated with saline or GSH-EE at p7 every 12 h for 6 weeks were processed for mass spectrometry analyses of ceramide (**A**); sphingomyelin (**B**); monohexosides (**C**); dihexosides (**D**) species and sphingosine (**E**) levels. Values are the mean ± SEM of 5 mice per group. $P < 0.05$ vs. *Npc1*$^{+/+}$ or *Npc1*$^{-/-}$ samples as indicated.

[37]. These findings along with our observations suggest that the neurological alterations rather than the liver phenotype determine the overall progression of the juvenile form of the disease. Moreover, our findings indicate that GSH-EE treatment does not affect the lipidomic profile of most sphingolipid species in liver and brain of *Npc1*$^{-/-}$ mice, except for specific sphingomyelin and monohexosylceramide species in brain of *Npc1*$^{-/-}$ mice. However, the relevance of the latter findings remains to be further investigated, as the role of the disruption of sphingolipid homeostasis in NPC disease is poorly understood. For instance, although accumulation of gangliosides, especially GM2 and GM3, has been reported in brain of *Npc1*$^{-/-}$ mice [6], GM3 synthase deletion has been shown to worsen NPC disease resulting in accelerated premature death of *Npc1*$^{-/-}$ mice despite decreasing GM3 levels [44]. In light of these findings, it seems unlikely that the effect of GSH-EE in the normalization of specific brain sphingolipid species may have contributed to the improvement in the neurological phenotype and increased survival of *Npc1*$^{-/-}$ mice.

Currently, there are no FDA-approved treatments for NPC disease. Given the promising effects of GSH-EE shown here and exploiting the fact that it crosses the blood brain barrier, it may be worth exploring its clinical use alone or in combination with other therapies that have shown beneficial effects in NPC pathology, including curcumin, which significantly attenuated NPC pathology and extended survival by 30% in *Npc1*$^{-/-}$ mice by restoring intracellular sphingosine unbalance and cytosolic calcium homeostasis [36], ibuprofen [13], chronic administration of HDAC inhibitors [45], or miglustat [6,35], which inhibits GCS and has been approved in Europe for the treatment of NPC patients. Of note, miglustat or Genz-529468, a more effective GCS inhibitor, have been shown to significantly delay motor impairment and premature death in *Npc1*$^{-/-}$ mice despite increased brain glucosylceramide levels [35], suggesting these inhibitors have off-target effects likely targeting the non-lysosomal glucosylceramidase. Moreover, although cholesterol-lowering approaches such as cholestyramine, statins and a low-cholesterol diet are ineffective in modifying the neurological progression of the disease [46,47], CDX, a cholesterol-extracting agent, exhibits promising effects in ameliorating NPC pathology. CDX contains a hydrophilic exterior and a hydrophobic interior allowing it to increase the solubility of poorly water-soluble molecules such as cholesterol. CDX has been reported to remove cholesterol from cultured cells [48,49], while intraperitoneal or subcutaneous CDX administration to *Npc1*$^{-/-}$ mice decreased free cholesterol storage in liver and delayed the onset of neurological disease, increased Purkinje cell survival and extended life span [34,50]. However, as CDX does not readily cross the blood brain barrier [51], the therapeutic efficacy of intraperitoneal or subcutaneous CDX administration in ameliorating NPC symptoms is puzzling. Therefore, since recent findings indicated that the intracisternal CDX administration prevents cerebellar dysfunction and delays premature death in feline NPC disease [52], it may be worth investigating whether GSH-EE combined with intrathecal injection of CDX via lumbar puncture may exhibit a potentiating effect in the treatment of NPC disease. Although to our knowledge there are no studies addressing the suitability of GSH-EE treatment for human therapy, the present findings suggest this approach may be worth exploring in patients with NPC disease.

In summary, the present findings provide new insights on the pathogenesis of this lysosomal storage disorder, with the identification of mGSH depletion as an important player. In addition, since mitochondrial cholesterol increase causes the depletion of mGSH, further understanding the mechanism underlying the accumulation of cholesterol in mitochondria may be of relevance in NPC disease. In this regard, we have observed increased expression of StARD1 levels in liver and brain of *Npc1*$^{-/-}$ mice by an ER stress-independent mechanism, and this outcome is accompanied by a significant upregulation of MLN64 (Torres et al, manuscript in preparation). Given the known functions of these proteins in intracellular cholesterol trafficking [53,54], these findings suggest that StARD1 and MLN64 could account for the accumulation of cholesterol in mitochondria and the expected mGSH depletion.

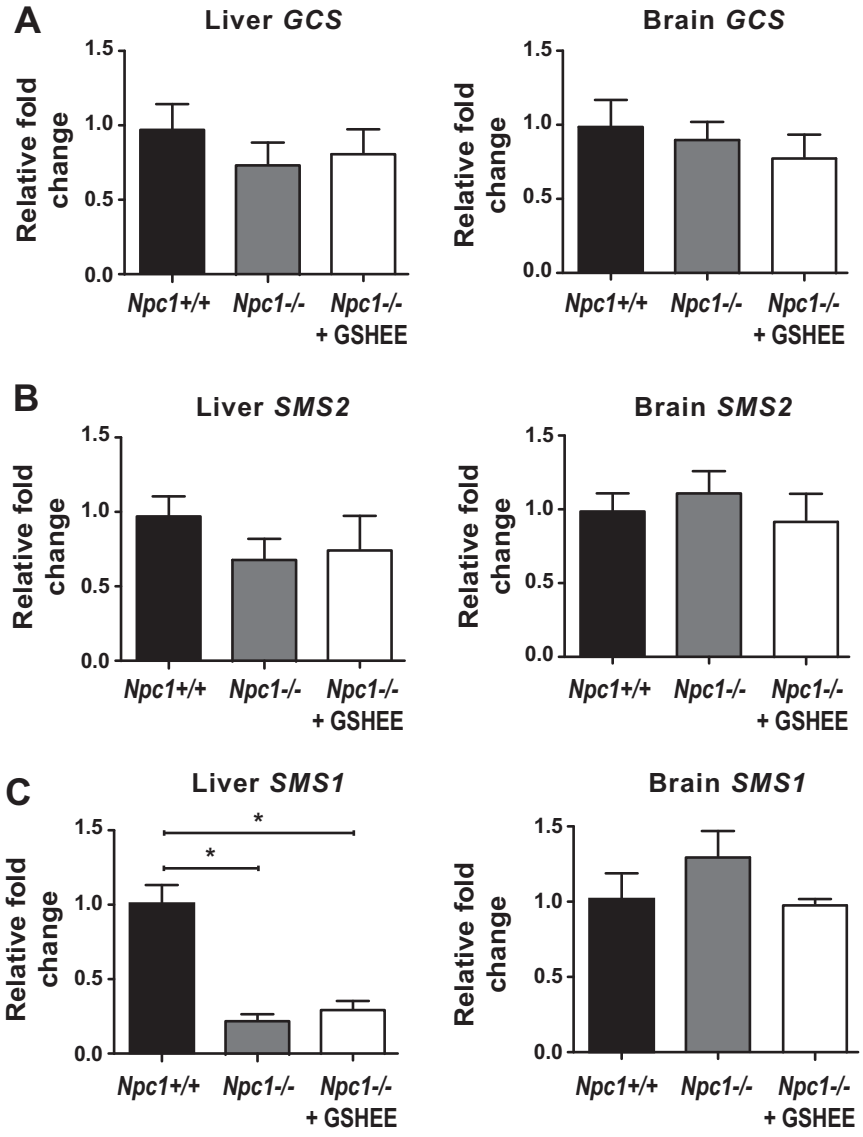

Fig. 7. Expression of GCS, SMS1 and SMS2 in liver and brain of Npc1-/- mice. Liver and brain samples from *Npc1*$^{+/+}$ mice and *Npc1*$^{-/-}$ mice treated with saline or GSH-EE at p7 every 12 h were processed for the determination of mRNA levels of GCS (**A**), SMS2 (**B**), SMS1 (**C**). Values are the mean ± SD of 5 mice per group. P < 0.05 vs. *Npc1*$^{+/+}$ samples.

Funding

The work was supported by grants SAF-2014-57674-R, SAF-2015-69944-R from Plan Nacional de I+D, Spain, Fundació Marató de TV3, La Mutua Madrileña, PI11/0325 (META) grant from the Instituto Salud Carlos III, and by the support of CIBEREHD; the center grant P50-AA-11999 Research Center for Liver and Pancretic Diseases funded by NIAAA/NIH; and support from AGAUR of the Generalitat de Catalunya 2014-SGR785.

Competing interests

The authors declare no competing financial interests.

Acknowledgments

We want to thank Drs. Vicente Ribas and Fabian Arenas for helpful discussions.

Appendix A. Supporting information

Supplementary data associated with this article can be found in the online version at doi:10.1016/j.redox.2016.11.010.

References

[1] E.P. Beltroy, J.A. Richardson, J.D. Horton, S.D. Turley, J.M. Dietschy, Cholesterol accumulation and liver cell death in mice with Niemann-Pick type C disease, Hepatology 42 (2005) 886–893.
[2] M.C. Patterson, C.J. Hendriksz, M. Walterfang, F. Sedel, M.T. Vanier, F. Wijburg, NP-C Guidelines Working Group. Recommendations for the diagnosis and management of Niemann-Pick disease type C: an update, Mol. Genet Metab. 106 (2012) 330–344.
[3] A.I. Rosenbaum, F.R. Maxfield, Niemann-Pick type C disease: molecular mechanisms and potential therapeutic approaches, J. Neurochem. 116 (2011) 789–795.
[4] M.T. Vanier, Complex lipid trafficking in Niemann-Pick disease type C, J. Inherit. Metab. Dis. 38 (2015) 187–199.
[5] H.J. Kwon, L. Abi-Mosleh, M.L. Wang, J. Deisenhofer, J.L. Goldstein, M.S. Brown, R.E. Infante, Structure of N-terminal domain of NPC1 reveals distinct subdomains for binding and transfer of cholesterol, Cell 137 (2009) 1213–1224.
[6] M. Fan, R. Sidhu, H. Fujiwara, B. Tortelli, J. Zhang, C. Davidson, S.U. Walkley, J.H. Bagel, C. Vite, N.M. Yanjanin, et al., Identification of Niemann-Pick C1 disease biomarkers through sphingolipid profiling, J. Lipid Res. 54 (2013) 2800–2814.
[7] R. Fu, C.A. Wassif, N.M. Yanjanin, D.E. Watkins-Chow, L.L. Baxter, A. Incao, L. Liscum, R. Sidhu, S. Firnkes, M. Graham, et al., Efficacy of N-acetylcysteine in phenotypic suppression of mouse models of Niemann-Pick disease, type C1, Hum. Mol. Genet. 22 (2013) 3508–3523.
[8] B.E. Kennedy, C.T. Madreiter, N. Vishnu, R. Malli, W.F. Graier, B. Karten, Adaptations of energy metabolism associated with increased levels of mitochondrial

cholesterol in Niemann-Pick type C1-deficient cells, J. Biol. Chem. 289 (2014) 16278–16289.
[9] M. Woś, J. Szczepanowska, S. Pikuła, A. Tylki-Szymańska, K. Zabłocki, J. Bandorowicz-Pikuła, Mitochondrial dysfunction in fibroblasts derived from patients with Niemann-Pick type C disease, Arch. Biochem. Biophys. 593 (2016) 50–59.
[10] W. Yu, J.-S. Gong, M. Ko, W.S. Garver, K. Yanagisawa, M. Michikawa, Altered cholesterol metabolism in Niemann-Pick type C1 mouse brains affects mitochondrial function, J. Biol. Chem. 280 (2005) 11731–11739.
[11] R. Fu, N.M. Yanjanin, S. Bianconi, W.J. Pavan, F.D. Porter, Oxidative stress in Niemann-Pick disease, type C, Mol. Genet. Metab. 101 (2010) 214–218.
[12] T. Marín, P. Contreras, J.F. Castro, D. Chamorro, E. Balboa, M. Bosch-Morató, F.J. Muñoz, A.R. Alvarez, S. Zanlungo, Vitamin E dietary supplementation improves neurological symptoms and decreases c-Abl/p73 activation in Niemann-Pick C mice, Nutrients 6 (2014) 3000–3017.
[13] D. Smith, K.-L. Wallom, I.M. Williams, M. Jeyakumar, F.M. Platt, Beneficial effects of anti-inflammatory therapy in a mouse model of Niemann-Pick disease type C1, Neurobiol. Dis. 36 (2009) 242–251.
[14] A. Fernández, L. Llacuna, J.C. Fernández-Checa, A. Colell, Mitochondrial cholesterol loading exacerbates amyloid beta peptide-induced inflammation and neurotoxicity, J. Neurosci. 29 (2009) 6394–6405.
[15] M. Marí, F. Caballero, A. Colell, A. Morales, J. Caballeria, A. Fernandez, C. Enrich, J.C. Fernandez-Checa, C. García-Ruiz, Mitochondrial free cholesterol loading sensitizes to TNF- and Fas-mediated steatohepatitis, Cell Metab. 4 (2006) 185–198.
[16] S.-D. Ha, S. Park, C.Y. Han, M.L. Nguyen, S.O. Kim, Cellular adaptation to anthrax lethal toxin-induced mitochondrial cholesterol enrichment, hyperpolarization, and reactive oxygen species generation through downregulating MLN64 in macrophages, Mol. Cell Biol. 32 (2012) 4846–4860.
[17] M. Marí, A. Morales, A. Colell, C. García-Ruiz, J.C. Fernández-Checa, Mitochondrial glutathione, a key survival antioxidant, Antioxid. Redox Signal 11 (2009) 2685–2700.
[18] A. Baulies, V. Ribas, S. Núñez, S. Torres, C. Alarcón-Vila, L. Martínez, J. Suda, M.D. Ybanez, N. Kaplowitz, C. García-Ruiz, et al., Lysosomal cholesterol accumulation sensitizes to acetaminophen hepatotoxicity by impairing mitophagy, Sci. Rep. 5 (2015) 18017.
[19] A.R. Alvarez, A. Klein, J. Castro, G.I. Cancino, J. Amigo, M. Mosqueira, L.M. Vargas, L.F. Yévenes, F.C. Bronfman, S. Zanlungo, Imatinib therapy blocks cerebellar apoptosis and improves neurological symptoms in a mouse model of Niemann-Pick type C disease, FASEB J. 22 (2008) 3617–3627.
[20] A. Colell, C. García-Ruiz, M. Miranda, E. Ardite, M. Marí, A. Morales, F. Corrales, N. Kaplowitz, J.C. Fernández-Checa, Selective glutathione depletion of mitochondria by ethanol sensitizes hepatocytes to tumor necrosis factor, Gastroenterology 115 (1998) 1541–1551.
[21] C. García-Ruiz, A. Colell, A. Morales, J.C. Fernandez-Checa, Defective TNF-alpha-mediated hepatocellular apoptosis and liver damage in acidic sphingomyelinase knockout mice, J. Clin. Invest. 111 (2003) 197–208.
[22] C. von Montfort, N. Matias, A. Fernandez, R. Fucho, L. Conde de la Rosa, M.L. Martinez-Chantar, J.M. Mato, K. Machida, H. Tsukamoto, M.P. Murphy, et al., Mitochondrial GSH determines the toxic or therapeutic potential of superoxide scavenging in steatohepatitis, J. Hepatol. 57 (2012) 852–859.
[23] C. García-Ruiz, A. Morales, A. Colell, A. Ballesta, J.C. Fernandez-Checa, Feeding S-adenosyl-L-methionine attenuates both ethanol-induced depletion of mitochondrial glutathione and mitochondrial dysfunction in periportal and perivenous rat hepatocytes, Hepatology 21 (1995) 207–214.
[24] J. Garcia, D. Han, H. Sancheti, L.-P. Yap, N. Kaplowitz, E. Cadenas, Regulation of mitochondrial glutathione redox status and protein glutathionylation by respiratory substrates, J. Biol. Chem. 285 (2010) 39646–39654.
[25] M.A. Williams, R.H. McCluer, The use of Sep-Pak C18 cartridges during the isolation of gangliosides, J. Neurochem. 35 (1980) 266–269.
[26] V.S. Gross, H.K. Greenberg, S.V. Baranov, G.M. Carlson, I.G. Stavrovskaya, A.V. Lazarev, B.S. Kristal, Isolation of functional mitochondria from rat kidney and skeletal muscle without manual homogenization, Anal. Biochem. 418 (33) (2011) 213–223.
[27] J.M. Lluis, A. Colell, C. García-Ruiz, N. Kaplowitz, J.C. Fernández-Checa, Acetaldehyde impairs mitochondrial glutathione transport in HepG2 cells through endoplasmic reticulum stress, 124, 2003, 708–724, Gastroenterology 124 (2003) 708–724.
[28] J. Mårtensson, J.C. Lai, A. Meister, High-affinity transport of glutathione is part of a multicomponent system essential for mitochondrial function, Proc. Natl. Acad. Sci. USA 87 (1990) 7185–7189.
[29] E. Barbero-Camps, A. Fernández, L. Martínez, J.C. Fernández-Checa, A. Colell, APP/PS1 mice overexpressing SREBP-2 exhibit combined Aβ accumulation and tau pathology underlying Alzheimer's disease, Hum. Mol. Genet 22 (2013) 3460–3476.
[30] R. Varatharajalu, M. Garige, L.C. Leckey, Adverse signaling of scavenger receptor class B1 and PGC1s in alcoholic hepatosteatosis and steatohepatitis and protection by betaine in rat, Am. J. Pathol. 184 (2014) 2035–2044.
[31] J. Josekutty, J. Iqbal, T. Iwawaki, K. Kohno, M.M. Hussain, Microsomal triglyceride transfer protein inhibition induces endoplasmic reticulum stress and increases gene transcription via Ire1α/cJun to enhance plasma ALT/AST, J. Biol. Chem. 288 (2013) 14372–14383.
[32] V. Ribas, C. García-Ruiz, J.C. Fernández-Checa, Glutathione and mitochondria, Front Pharm. 5 (2014) 151.
[33] A. Jain, J. Mårtensson, E. Stole, P.A. Auld, A. Meister, Glutathione deficiency leads to mitochondrial damage in brain, Proc. Natl. Acad. Sci. USA 88 (1991) 1913–1917.
[34] C.D. Davidson, N.F. Ali, M.C. Micsenyi, G. Stephney, S. Renault, K. Dobrenis, D.S. Ory, M.T. Vanier, S.U. Walkley, Chronic cyclodextrin treatment of murine Niemann-Pick C disease ameliorates neuronal cholesterol and glycosphingolipid storage and disease progression, PLoS One 4 (2009) e6951.
[35] J.B. Nietupski, J.J. Pacheco, W.-L. Chuang, K. Maratea, L. Li, J. Foley, K.M. Ashe, C.G.F. Cooper, J.M.F.G. Aerts, Iminosugar-based inhibitors of glucosylceramide synthase prolong survival but paradoxically increase brain glucosylceramide levels in Niemann-Pick C mice, Mol. Genet. Metab. 105 (2012) 621–628.
[36] E. Lloyd-Evans, A.J. Morgan, X. He, D.A. Smith, E. Elliot-Smith, D.J. Sillence, G.C. Churchill, E.H. Schuchman, A. Galione, F.M. Platt, Niemann Pick type C1 disease is a sphingosine disease that causes deregulation of lysosomal calcium, Nat. Med. 14 (2008) 1247–1255.
[37] M. Bosch, A. Fajardo, R. Alcalá-Vida, A. Fernández-Vidal, F. Tebar, C. Enrich, F. Cardellach, E. Pérez-Navarro, A. Pol, Hepatic primary and secondary cholesterol deposition and damage in Niemann-Pick disease, Am. J. Pathol. 186 (2016) 517–523.
[38] J.J. Barski, J. Hartmann, C.R. Rose, F. Hoebeek, K. Mörl, M. Noll-Hussong, C.I. De Zeeuw, A. Konnerth, M. Meyer, Calbindin in cerebellar Purkinje cells is a critical determinant of the precision of motor coordination, J. Neurosci. 23 (2003) 3469–3477.
[39] F.D. Porter, D.E. Scherrer, M.H. Lanier, S.J. Langmade, V. Molugu, S.E. Gale, D. Olzeski, R. Sidhu, D.J. Dietzen, R. Fu, et al., Cholesterol oxidation products are sensitive and specific blood-based biomarkers for Niemann-Pick C1 disease, Sci. Transl. Med. 2 (2010) 56ra81.
[40] D.M. Guidot, L.A. Brown, Mitochondrial glutathione replacement restores surfactant synthesis and secretion in alveolar cells of ethanol-fed rats, Alcohol Clin. Exp. Res 24 (2000) 1070–1076.
[41] A. Louvet, P. Mathurin, Alcoholic liver disease: mechanisms of injury and targeted treatment, Nat. Rev. Gastroenterol. Hepatol. 12 (2015) 231–242.
[42] M. Mari, A. Morales, A. Colell, C. Garcia-Ruiz, J.C. Fernandez-Checa, Mitochondrial cholesterol accumulation in alcoholic liver disease: role of ASMase and endoplasmic reticulum stress, Redox Biol. 3 (2014) 100–108.
[43] M.C. Vázquez, T. del Pozo, F.A. Robledo, G. Carrasco, L. Pavez, F. Olivares, M. González, S. Zanlungo, Alteration of gene expression profile in Niemann-Pick type C mice correlates with tissue damage and oxidative stress, PLoS One 6 (2011) e28777.
[44] B. Liu, H. Li, J.J. Repa, S.D. Turley, J.M. Dietschy, Genetic variations and treatment that affect the lifespan of the NPC1 mouse, J. Lipid Res 49 (2008) 663–669.
[45] M.S. Alam, M. Getz, K. Haldar, Chronic administration of an HDAC inhibitor treats both neurological and systemic Niemann-Pick type C disease in a mouse model, Sci. Transl. Med. 8 (2016) (326ra23).
[46] M.C. Patterson, A.M. Di Bisceglie, J.J. Higgins, R.B. Abel, R. Schiffmann, C.C. Parker, C.E. Argoff, R.P. Grewal, K. Yu, P.G. Pentchev, The effect of cholesterol-lowering agents on hepatic and plasma cholesterol in Niemann-Pick disease type C, Neurology 43 (1993) 61–64.
[47] K.L. Somers, D.E. Brown, R. Fulton, P.C. Schultheiss, D. Hamar, M.O. Smith, R. Allison, H.E. Connally, C. Just, T.W. Mitchell, et al., Effects of dietary cholesterol restriction in a feline model of Niemann-Pick type C disease, J. Inherit. Metab. Dis. 24 (2001) 427–436.
[48] V.M. Atger, M. de la Llera Moya, G.W. Stoudt, W.V. Rodrigueza, M.C. Phillips, G.H. Rothblat, Cyclodextrins as catalysts for the removal of cholesterol from macrophage foam cells, J. Clin. Invest. 99 (1997) 773–780. http://dx.doi.org/10.1172/JCI119223.
[49] S.M. Liu, A. Cogny, M. Kockx, R.T. Dean, K. Gaus, W. Jessup, L. Kritharides, Cyclodextrins differentially mobilize free and esterified cholesterol from primary human foam cell macrophages, J. Lipid Res. 44 (2004) 1156–1166.
[50] B. Liu, S.D. Turley, D.K. Burns, A.M. Miller, J.J. Repa, J.M. Dietschy, Reversal of defective lysosomal transport in NPC disease ameliorates liver dysfunction and neurodegeneration in the npc1-/- mouse, Proc. Natl. Acad. Sci. USA 106 (2009) 2377–2382.
[51] C.C. Pontikis, C.D. Davidson, S.U. Walkley, F.M. Platt, D.J. Begley, Cyclodextrin alleviates neuronal storage of cholesterol in Niemann-Pick C disease without evidence of detectable blood-brain barrier permeability, J. Inherit. Metab. Dis. 36 (2013) 491–498.
[52] C.H. Vite, J.H. Bagel, G.P. Swain, M. Prociuk, T.U. Sikora, V.M. Stein, P. O'Donnell, T. Ruane, S. Ward, A. Crooks, et al., Intracisternal cyclodextrin prevents cerebellar dysfunction and Purkinje cell death in feline Niemann-Pick type C1 disease, Sci. Transl. Med. 7 (2015) 276ra26.
[53] W.L. Miller, Disorders in the initial steps of steroid hormone synthesis, J. Steroid Biochem. Mol. Biol. (2016) 6.
[54] M. Charman, B.E. Kennedy, N. Osborne, B. Karten, MLN64 mediates egress of cholesterol from endosomes to mitochondria in the absence of functional Niemann-Pick Type C1 protein, J. Lipid Res. 51 (2010) 1023–1034.